JOURNAL OF GEOPHYSICAL RESEARCH, VOL. 107, NO. E10, 5082, doi:10.1029/2000JE001474, 2002

Survival of impact-induced thermal anomalies in the Martian mantle

C. C. Reese[1] and V. S. Solomatov
Department of Physics, New Mexico State University, Las Cruces, New Mexico, USA

J. R. Baumgardner
Theoretical Division, Los Alamos National Laboratory, Los Alamos, New Mexico, USA

Received 16 February 2001; revised 15 November 2001; accepted 22 April 2002; published 23 October 2002.

[1] A number of geophysical arguments point out the possibility that global mantle convection could have been extremely sluggish or even absent during a large part of Martian history. This implies that early mantle thermal anomalies produced during planetary formation might not have been quickly erased by vigorous convection. One likely mechanism of early thermal inhomogeneity is large impacts at the end of heavy bombardment. We suggest that Tharsis province might be related to such an impact-induced thermal anomaly rather than a convective plume. The shape of the present-day geoid for our preferred model is in good agreement with the geoid measured by Mars Global Surveyor (MGS). *INDEX TERMS:* 6225 Planetology: Solar System Objects: Mars; 5430 Planetology: Solid Surface Planets: Interiors (8147); 5455 Planetology: Solid Surface Planets: Origin and evolution; 5417 Planetology: Solid Surface Planets: Gravitational fields (1227); *KEYWORDS:* Martian mantle convection, Martian thermal evolution, impact heating, origin of Tharsis, Martian geoid

Citation: Reese, C. C., V. S. Solomatov, and J. R. Baumgardner, Survival of impact-induced thermal anomalies in the Martian mantle, *J. Geophys. Res.*, *107*(E10), 5082, doi:10.1029/2000JE001474, 2002.

1. Introduction

[2] The initial thermal state of Mars was likely heterogeneous as a result of the stochastic nature of planetary formation including large impacts, iron core segregation and early internal dynamics. Impacts of large planetesimals [*Wetherill*, 1980, 1990; *Weidenschilling et al.*, 1997; *Agnor et al.*, 1999] during late-stage Mars formation can locally shock heat the deep mantle to supersolidus temperatures [*Melosh*, 1990; *Tonks and Melosh*, 1992, 1993; *Pierazzo et al.*, 1997]. Potential energy release via core formation [e.g., *Solomon*, 1979] might result in additional localized heating. It has also been suggested that an early phase of internal dynamics produced an asymmetrical mode of heat loss [*Zuber et al.*, 2000] which cooled the mantle beneath the northern lowlands. This hypothesis implies thermal heterogeneity on the largest ($\sim$hemispheric) scale. In this study we investigate the thermal evolution of Mars with initial thermal heterogeneity produced by impact heating. The fate of early thermal heterogeneities depends on the nature of mantle convection. If convection is vigorous mantle anomalies are quickly eliminated while if convection is sluggish and heat transfer is inefficient heterogeneities can persist throughout planetary evolution. New data and an improved understanding of interior processes seem to support the hypothesis of sluggish convection and inefficient thermal homogenization of the mantle. In the absence of a convective plume, we suggest that Tharsis might be related to a long-lived, impact-induced thermal anomaly preserved because of sluggish or no convection.

2. Observations

2.1. Initial Condition

[3] Core formation and the initial thermal structure of Mars is an unresolved problem. While it was once thought that Martian core formation may have been delayed [*Solomon and Chaiken*, 1976], it is now well established that the core formed early, within $\sim$30 Myr of the beginning of the Solar System [*Lee and Halliday*, 1997]. Early core formation has been interpreted as implying a hot (near solidus) initial state [*Schubert et al.*, 1992] because models of metal–silicate separation require a partially molten mantle [*Stevenson*, 1981, 1990; *Karato and Murthy*, 1997]. On the other hand, if accreting planetesimals are cold, growing protoplanet interiors are cold (energy of formation scales with accreting body radius squared) and melting occurs near the surface only when the mass reaches $\sim$0.1 Earth masses [*Safronov*, 1978; *Kaula*, 1979; *Coradini et al.*, 1983; *Abe and Matsui*, 1985; *Sasaki and Nakazawa*, 1986; *Zahnle et al.*, 1988] which is about the mass of Mars. However, decay of short-lived radioactive isotopes, most notably aluminum-26 [e.g., *Grimm and McSween*, 1993], can result in significant heating of planetesimal interiors [*Keil*, 2000]. Recently, it has been pointed out that several mechanisms, in addition to metal sinking through molten silicates, can contribute to core formation [*Rushmer et al.*, 2000]. In fact, experimental studies suggest that the Martian core could form without extensive silicate melting [*Bruhn et al.*, 2000; *Gaetani and Grove*, 1997]. In any case, core formation would increase

[1]Now at University of Minnesota at Morris, Morris, Minnesota 56267, USA.

0148-0227/02/2000JE001474$09.00

the average interior temperature of Mars by only ~300 K [*Solomon*, 1979].

2.2. Plate Tectonics?

[4] The question of whether Mars ever had plate tectonics is controversial. It has been suggested that early Mars evolved via an analog of plate tectonics and that the northern lowlands formed in the final stages of that transient episode [*Sleep*, 1994]. However, *Pruis and Tanaka* [1995] argued that there is not much evidence to support this hypothesis and that many geological structures have incorrect orientations. The magnetometer experiment on Mars Global Surveyor (MGS) detected a remnant crustal magnetic field in the southern highlands of large magnitude [*Acuña et al.*, 1999; *Purucker et al.*, 2000]. The magnetic anomalies appear to have formed before major impacts since Argyre and Hellas seem to have destroyed magnetization. This requires an early and vigorous Martian dynamo implying efficient planetary cooling to allow convection in the core [*Stevenson et al.*, 1983; *Nimmo and Stevenson*, 2000]. The observed features have been interpreted as a possible feature of spreading center processes [*Connerney et al.*, 1999] and *Zuber et al.* [2000] point out that a distinct northern lowland internal structure inferred from gravity and topography, also postulated to be a region of high heat flux, corresponds closely to the margins of late-stage mobile plates proposed by *Sleep* [1994]. On the other hand, alternative mechanisms are possible [*Connerney et al.*, 1999; *Nimmo*, 2000; *Raymond et al.*, 2000]. If plate tectonics did occur on Mars, its duration should have been no more than a few hundred million years, as indicated by surface ages as well as ^{40}Ar degassing models [*Tajika and Sasaki*, 1996]. Subsequent mantle convection probably occurs in the stagnant lid regime (see below) characterized by slow convective velocities and inefficient heat transfer. Finally, isotopic evidence from shergottites indicates a geochemically heterogeneous Martian mantle arguing against extensive mixing by vigorous convection [*Albarède et al.*, 2000].

2.3. Mantle Water Content

[5] There is ubiquitous geological evidence for liquid water at the surface in the past [e.g., *Baker et al.*, 1992; *Carr*, 1996; *Head et al.*, 1999] and it has been suggested that liquid water may even be present today [*Malin and Edgett*, 2000]. On the other hand, several estimates of SNC meteorite water content suggest levels about one order of magnitude lower than typical MORB [*Fallick et al.*, 1983; *Yang and Epstein*, 1985; *Kerridge*, 1988; *Karlsson et al.*, 1992]. One possibility is that primordial water reacted with reduced iron prior to core formation producing hydrogen which was subsequently lost [*Dreibus and Wänke*, 1987] resulting in a relatively dry mantle. In this case, the geological and geochemical evidence can be reconciled by delivery of a late veneer of volatile rich material and inefficient recycling into the mantle [*Carr and Wänke*, 1992]. However, there is evidence from SNC melt inclusions suggesting a mantle water content similar to that of terrestrial mantle [*Johnson et al.*, 1991; *McSween and Harvey*, 1993]. Outgassing of water associated with volcanism [e.g., *Greeley*, 1987] may have contributed to formation of ancient fluvial features. If the Martian interior was initially water poor or sufficiently devolatilized early in planetary history, the mantle may have been relatively dry and viscous compared to terrestrial upper mantle.

2.4. Mantle Mineralogy

[6] Recent models of the chemical and mineralogical composition of Mars [*Bertka and Fei*, 1998a, 1998b], demonstrate that a C1 chondritic Fe abundance and Fe/Si ratio is inconsistent with the new and improved moment of inertia value, 0.3662 ± 0.0017, from Mars Pathfinder data [*Folkner et al.*, 1997]. This led to the suggestion that a mixture of carbonaceous with ordinary and/or enstatite chondrites might yield a composition more consistent with observations [*Bertka and Fei*, 1999]. Independently, an ordinary-enstatite chondrite mixture was proposed based on SNC oxygen isotopes [*Sanloup et al.*, 1999]. In both cases reduced Mg/Si ratios imply a large pyroxene/olivine ratio. The latter model predicts that pyroxene is the dominant mantle mineral assemblage. Although wet pyroxene can be as weak or weaker than wet olivine, dry pyroxene is stronger than dry olivine (see below).

3. Martian Mantle Convection

3.1. Constant Versus Temperature-Dependent Viscosity

[7] The first calculations of Martian convective stability were based on constant viscosity criteria [*Schubert et al.*, 1969; *Tozer*, 1972]. The stability condition for a constant viscosity, internally heated fluid layer is that the Rayleigh number based on the heating rate be greater than the critical Rayleigh number. For typical Mars parameters (Table 1), no-slip velocity boundary conditions, and a present-day chondritic heating rate, the Martian mantle would be convectively unstable if the viscosity were less than ~10^{25} Pa s. Because this value is large (i.e., much greater than estimates of terrestrial upper mantle viscosity), it was concluded that the Martian mantle was indeed unstable and thermal convection would occur. In the constant viscosity case, the scaling relationship between convective heat transfer and internal temperature can be written as

$$F(T_i) = \frac{k(T_i - T_s)}{d}\; a\,\mathrm{Ra}^{\beta}, \qquad (1)$$

where T_i and T_s are the interior and surface temperatures, respectively, Ra is the Rayleigh number based on the temperature difference across the layer

$$\mathrm{Ra} = \frac{g\rho\alpha(T_i - T_s)d^3}{\kappa\eta}, \qquad (2)$$

g is the acceleration due to gravity, ρ is the density, α is the coefficient of thermal expansion, d is the layer depth, κ is the thermal diffusivity, η is the dynamic viscosity, and a and β are constants that depend on the boundary conditions and weakly on the Rayleigh number itself. Boundary layer theory [*Turcotte and Oxburgh*, 1967] suggests a = 0.167 and β = 1/3. It was originally thought that the strong temperature dependence of silicate rock rheology would have a relatively minor effect on the heat flux–temperature relation (1). In this case, the viscosity based on the interior temperature can be substituted in the Rayleigh number,

$$\eta = \frac{1}{2A}\mu^n\left(\frac{h}{B}\right)^m \tau^{1-n}\exp\left(\frac{Q}{RT}\right), \qquad (3)$$

Table 1. Mars Parameters

Parameter	Notation	Value
Layer depth	d	1663 km
Thermal conductivity	k	4 W/m K
Thermal expansivity	α	2×10^{-5} K^{-1}
Density	ρ	3470 kg/m^3
Gravity	g	3.7 m/s^2
Thermal diffusivity	κ	9.6×10^{-7} m^2/s^1
Surface temperature	T_s	220 K

where A is the preexponential factor, μ is the shear modulus, n is the power law exponent, h is the grain size, B is the Burgers vector length, m is the grain size exponent, τ is the second invariant of the stress tensor, T is temperature, R is the gas constant, and $Q = E + pV$ where E is the activation energy, p is the pressure, V is the activation volume, $n \approx 1$ for diffusion creep, and $n \approx 3.0$–3.5 for dislocation creep [*Karato and Wu*, 1993]. Using (1) and the parameters of Tables 1 and 2, one can calculate the dependence of the Martian heat flux on internal temperature (Figure 1). This figure suggests that at modest interior temperatures (much less than the melting temperature) Mars is capable of removing internally generated heat. For a mantle heat flux corresponding to the present-day chondritic heating rate the temperature of the Martian mantle can vary from $\approx$1200 to 1600 K depending on the grain size.

[8] Temperature-dependent viscosity, however, completely changes the nature of thermal convection. In the asymptotic large viscosity variation regime the most viscous part of the lithosphere is essentially immobile and if convective instabilities develop, they do so only in a thin sublithospheric layer [*Morris and Canright*, 1984; *Fowler*, 1985; *Ogawa et al.*, 1991; *Davaille and Jaupart*, 1993; *Solomatov*, 1995; *Moresi and Solomatov*, 1995; *Doin et al.*, 1997; *Trompert and Hansen*, 1998; *Grasset and Parmentier*, 1998; *Solomatov and Moresi*, 2000]. The scaling relationship between convective heat flux and interior temperature in the stagnant lid regime can be written as

$$F(T_i) = \frac{k(T_i - T_s)}{d} a\theta^{-\zeta}\mathrm{Ra}_i^{\beta}, \tag{4}$$

where a, ζ, and β are constants that depend on n,

$$\theta = \frac{(T_i - T_s)E}{RT_i^2} - \frac{P_i V T_s}{RT_i^2}, \tag{5}$$

P_i is the pressure at the bottom of the lithosphere,

$$\mathrm{Ra}_i = \frac{g\rho\alpha(T_i - T_s)d^{(n+2)/n}}{c^{1/n}\kappa^{1/n}\exp[(E + P_i V)/nRT_i]}, \tag{6}$$

and

$$c = (1/2A)\mu^{n-1}(h/B)^m. \tag{7}$$

Systematic numerical simulations [*Solomatov and Moresi*, 2000] suggest that $a = (0.31 + 0.22n)$, $\zeta = -2(n+1)/(n+2)$ and $\beta = n/(n+2)$. The dependence of the heat flux on temperature is shown in Figure 2 for an olivine Martian mantle.

[9] A comparison of pyroxene and olivine rheologies is difficult due to the lack of data on pyroxene activation volume. Experimental data is also limited to deformation dominated by dislocation mechanisms ($n > 1$). We can compare the heat flux–temperature relation for olivine in dislocation creep to that of pyroxene rheologies assuming that the activation volumes are roughly the same (Figure 3). While wet enstatite [*Ross and Nielsen*, 1978] is weaker than wet olivine, dry single-crystal enstatite is somewhat stronger than dry olivine [*Mackwell*, 1991]. Furthermore, it has been noted (Karato, personal communication, 2000) that the strength of polycrystalline aggregates of pyroxene might be even higher relative to olivine because of the smaller number of slip systems. A polycrystalline websterite sample [*Avé Lallemant*, 1978] is much stronger than olivine for both wet and dry conditions.

3.2. Thermal Evolution

[10] As a first-order approximation we consider an initial condition consisting of a cold thermal boundary layer (lithosphere) over an isothermal mantle. In this case, the lithosphere itself becomes convectively unstable in the same manner that onset of convection occurs in a static layer heated from below. A convective regime diagram for Newtonian viscosity is shown in Figure 4 in terms of the Rayleigh number defined at the viscosity beneath the lithosphere, Ra_i, and the viscosity contrast across the lithosphere $\Delta\eta$. Also shown are two initial conditions (squares) corresponding to a lithospheric thickness of 50 km and interior temperatures of 1400 and 1800 K. In the constant viscosity case (along the x axis), both of these initial conditions are unstable and convection involves recycling of the entire lithosphere.

[11] In this case, the planetary energy budget can be written (neglecting the core) as

$$M_m c_p \frac{\partial T_i}{\partial t} = M_m H(t) - SF(T_i), \tag{8}$$

where M_m is the mass of the mantle, c_p is the heat capacity, $H(t)$ is the radiogenic heating rate which decays exponentially with time, S is the surface area, F is the heat flux, T_i is the internal temperature, and t is time. The heat flux parameterization based on constant viscosity convection (equation (1)) allows the planet to quickly self-regulate [*Tozer*, 1965]. Mars heats up if initially too cold and cools down if initially too hot [*Töksoz et al.*, 1978; *Schubert et al.*, 1979; *Turcotte et al.*, 1979; *Schubert and Spohn*, 1990; *Spohn*, 1991; *Schubert et al.*, 1992]. Adjustment from the initial condition to a state where heat loss balances internally generated heat and thermal cooling takes $\sim 10^9$

Table 2. Rheological Parameters

	Diffusion creep		Dislocation creep	
	Wet	Dry	Wet	Dry
A (s^{-1})	5.3×10^{15}	8.7×10^{15}	2.0×10^{18}	3.5×10^{22}
n	1.0	1.0	3.0	3.5
m	2.5	2.5	0.0	0.0
E (kJ/mol)	240	300	430	540
V (cm^3/mol)	5	6	10–20	15–25

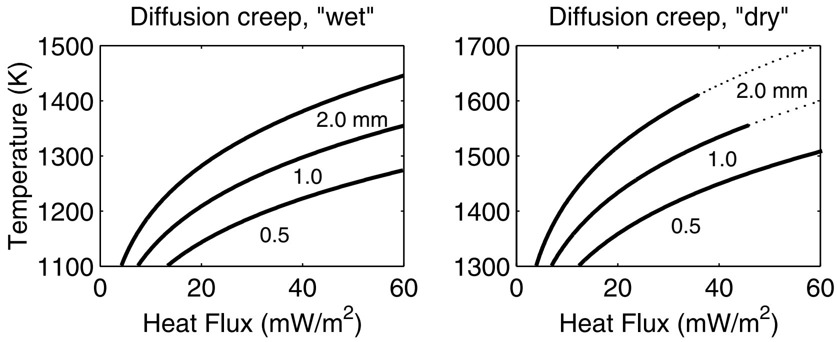

Figure 1. Mantle temperature as a function of heat flux for the scaling based on constant viscosity convection (1) and a rheology corresponding to diffusion creep (n = 1, m = 2.5) of "wet" and "dry" olivine (see Table 1) [*Karato and Wu*, 1993]. Curves are labeled by grain size h, and the length of the Burgers vector is B = 0.5 nm. The dotted line indicates that the mantle is partially molten.

years. Subsequently, Mars thermal history is characterized by subsolidus cooling of ~100 K (Figure 5).

[12] For a rheological law corresponding to wet olivine in diffusion creep, the formal location of the initial conditions (Figure 4) are shown in the Frank–Kamenetskii approximation [e.g., *Reese et al.*, 1999b]. The viscosity contrast across the lithosphere for the Arrhenius viscosity law is many orders of magnitude larger, but has little effect on the heat flux. In this case, both initial conditions are convectively stable and the lithosphere thickens conductively while the interior heats up. Onset of convection is delayed and when instabilities develop, they do so in the stagnant lid regime. Thus, whether an initial mantle temperature near solidus is sufficient to initiate stagnant lid convection depends on deformation mechanism, grain size, mineralogy, and water content. It is possible, even for initial temperatures near solidus, that a dry Martian mantle might have to heat up (accompanied by further melting) before convection can start.

[13] The most profound consequence of the heat flux parameterization based on stagnant lid convection (equation (4)) is substantially higher mantle temperatures than predicted by constant viscosity models. Establishment of the self-regulated state can take ~3–4 Gyr and Mars thermal history is characterized by heating for much of evolution. In fact, stagnant lid convection cannot maintain a subsolidus mantle (Figure 6). The prediction of supersolidus mantle temperatures for the majority of Martian evolution (Figure 6)

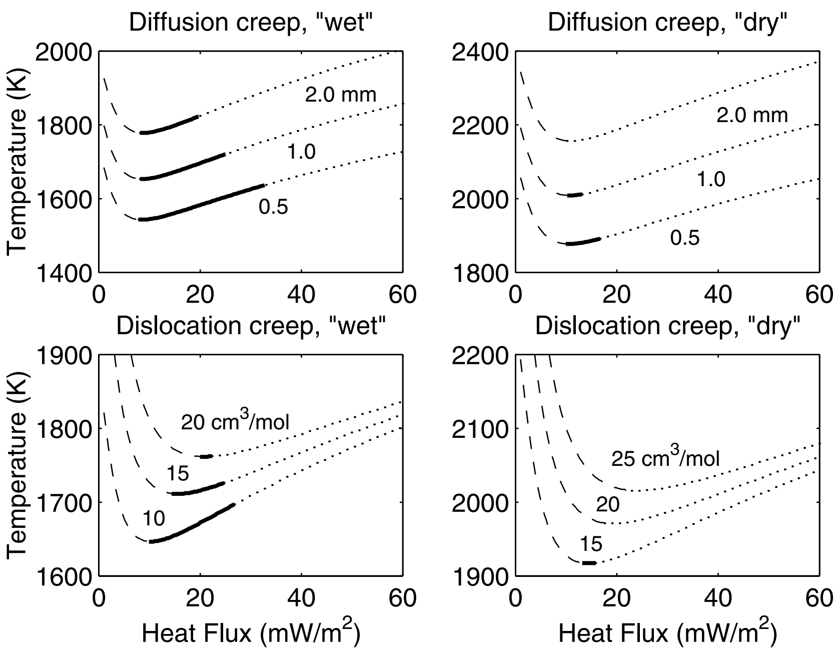

Figure 2. Mantle temperature in the stagnant lid convection regime (4) for diffusion (n = 1, m = 2.5) and dislocation creep (n = 3 (wet), n = 3.5 (dry), m = 0) of "wet" and "dry" olivine (see Table 1). For diffusion and dislocation creep, curves are labeled by grain size and activation volume, respectively. For a given temperature, there are stable (solid line) and unstable (dashed line) solutions as a consequence of pressure-dependent viscosity [*Reese et al.*, 1999b]. The dotted line indicates that the mantle is partially molten.

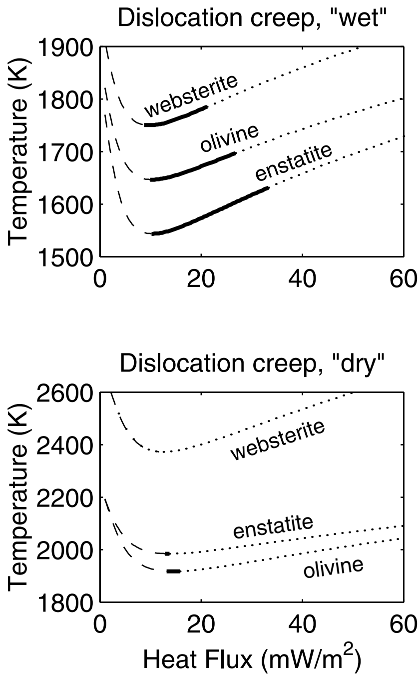

Figure 3. A comparison of olivine and pyroxene rheologies. The dry enstatite is a single-crystal sample in the protoenstatite stability field oriented for creep on the weakest slip-system, and the wet enstatite (0.89 enstatite, 0.08 fosterite, and 0.03 wollastonite) and websterite (0.68 cpx, 0.32 opx) are polycrystalline. The olivine curves correspond to the lower activation volume limits, 10 and 15 cm^3/mol, respectively.

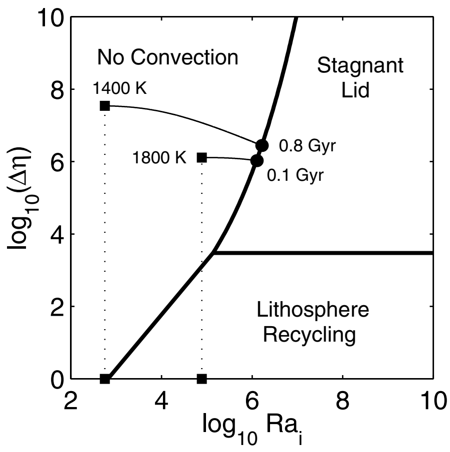

Figure 4. Convective regimes in interior Rayleigh number–lithospheric viscosity contrast space. The boundary for the onset of convection (thick line) is divided into a lower branch where the entire lithosphere participates in convection and an upper branch where convection occurs in the stagnant lid regime. The initial conditions for a 50 km lithosphere and interior temperatures of 1400 and 1800 K are shown by squares. In the constant viscosity case (along the *x* axis), both initial conditions are convectively unstable and the whole lithosphere is recycled. For the rheological law corresponding to wet olivine in diffusion creep, the formal location of the initial conditions are shown in the Frank–Kamenetskii approximation. In this case, both initial conditions are convectively stable and the lithosphere thickens conductively while the interior heats up (thin line). The onset of convection (solid circles, time in Gyr) is delayed and instabilities develop in the stagnant lid regime.

is at odds with the fact that much of the surface is old [e.g., *Hauck and Phillips*, 2000]. Southern highland stabilization records the termination of heavy bombardment and Tharsis development dates to early planetary evolution (see below). Estimates of the volcanic flux suggest an evolution from higher rates and widespread activity to lower rates and more localized activity [e.g., *Tanaka et al.*, 1992].

[14] It was suggested that volcanism and extensive differentiation of heat-producing elements into the crust is one way Mars might respond to widespread melting in the stagnant lid regime [*Reese et al.* 1998]. Differentiation lowers the internal heat production rate and mantle temperature, preventing further melting and reducing the vigor of convection [*Turcotte*, 1989; *Spohn*, 1991; *Schubert et al.*, 1992]. Water depletion accompanying melt extraction also prevents melting by considerably raising the solidus of peridotites [*Thompson*, 1992] and reduces convective vigor by increasing the viscosity [*Karato*, 1986]. In fact, accounting for differentiation (Appendix A) suggests that stagnant lid convection may only last ~1–2 Gyr (Figure 7). Differentiation could also result in compositional stratification of the mantle which tends suppress convection.

4. Tharsis

[15] A particularly important constraint on Mars thermal history is the origin of Tharsis province, a broad topographic bulge comprised of regional centers of tectonism and volcanism [*Anderson et al.*, 1998; *Dohm et al.*, 2000]. Large variations in crustal structure [*Zuber et al.*, 2000] and observations of layered materials ~8 km thick at the margins of Valles Marineris [*McEwen et al.*, 1999] support the suggestion that constructional volcanism is partially responsible for the elevation of Tharsis [*Solomon and Head*, 1982]. Some of the thickest crust is associated with old centers of volcanic activity such as Syria Planum and Thaumasia [*Solomon et al.*, 2000]. Faulting patterns dating to the Noachian are consistent with a flexural loading model

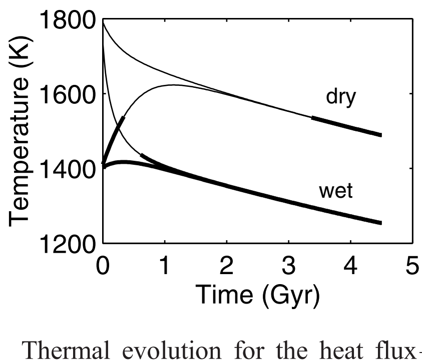

Figure 5. Thermal evolution for the heat flux–temperature scaling based on constant viscosity (equation (1) and Figure 1) and a grain size of 1 mm. The thin line indicates that the mantle is partially molten. The evolution is dominated by convective cooling and early establishment of the self-regulated state.

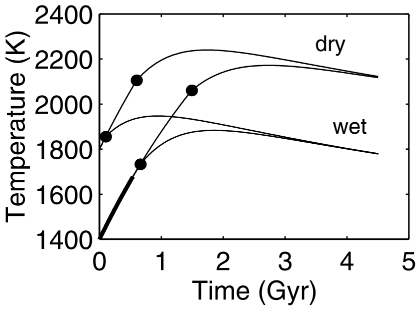

Figure 6. Thermal evolution in the stagnant lid regime (equation (4) and Figure 2) for diffusion creep with a grain size of 1 mm (dislocation creep gives similar results). The thin line indicates that the mantle is partially molten and circles indicate the onset of lithospheric instabilities (Figure 4). The thermal evolution is dominated by heating and even for "wet" conditions the mantle is molten for most of planetary history.

based on present-day topography and gravity suggesting that the Tharsis load was emplaced by ~3 Gyr ago [*Banerdt and Golombek*, 2000]. A topographic trough surrounding Tharsis, suggested to be due to flexural downwarp of the lithosphere, appears to have focused ancient fluvial activity [*Phillips et al.*, 2000]. These observations suggest that vigorous magmatic activity and Tharsis development dates to the earliest part of the Martian geological record and that this activity decreased with time but continued at low levels to essentially the present-day [*Hartmann et al.*, 1999a, 1999b].

4.1. Mantle Plume Hypothesis

[16] Within the paradigm of vigorous Martian mantle convection, the monopolar distribution of tectonism and younger volcanism at Tharsis led to the suggestion that the pattern of convection on Mars is characterized by one large upwelling [*Hartmann*, 1973; *Carr*, 1974; *Phillips and Ivins*, 1979]. This could be due to a hot plume originating at the core–mantle boundary like on Earth but much bigger. At first, this hypothesis faced problems since convection models based on constant viscosity predicted too many plumes [*Schubert and Spohn*, 1990; *Schubert et al.*, 1992] Further studies discovered that a one-plume planform of convection on Mars can be caused by mineralogical phase transformations in the deep mantle [*Weinstein*, 1995; *Harder and Christensen*, 1996; *Breuer et al.*, 1998; *Spohn et al.*, 1998; *Harder*, 2000].

[17] If Mars evolves in the stagnant lid regime, formation of a plume could be problematic because of mantle heating (Figures 6 and 7). Although a transient episode of early surface recycling can facilitate mantle cooling, the inevitable subsequent transition to stagnant lid convection changes the mode of evolution from cooling to heating shutting off the core heat flux and associated plume activity [*Nimmo and Stevenson*, 2000].

4.2. An Alternative Hypothesis

[18] A particularly striking feature of Tharsis is the circular nature of the associated geoid anomaly [*Smith et al.*, 1999b] in contrast to the complex topography [*Smith et al.*, 1999a] and gravity [*Zuber et al.*, 2000] of the region. We hypothesize that an alternative mechanism capable of producing such a circular geoid anomaly, other than a highly symmetric megaplume, is a large impact. However, there is no present-day geophysical evidence for a large impact at Tharsis [*Zuber et al.*, 2000]. Although pre-MGS geological mapping was interpreted as revealing highly modified basin remnants within and around Tharsis [*Schultz and Glicken*, 1979; *Schultz*, 1984; *Schultz and Frey*, 1990], major impact basins identified on the basis of MGS topography and gravity data only include Hellas, Utopia and Isidis [*Smith et al.*, 1999a, 1999b].

[19] On the other hand, models of Mars formation suggest that there might be impacts larger than that which formed the Hellas basin. The mass spectrum of planetesimals which accumulated to form Mars is likely approximated by a power law, $n(m) \sim m^{-\alpha}$, where $n(m)$ dm is the number of bodies with mass between m and $m + dm$. In many models [e.g., *Wetherill*, 1980] the exponent α lies between limiting values of 5/3 (each mass decade contributes equally to the total surface area) and 2 (each mass decade contributes equally to the total mass). Example planetesimal inventories in these limiting cases are shown for Mars in Figure 8. The important point is not the particular numbers of planetesimals in these end-member cases but rather that large impacts are inevitable during accretion. The hypothesis is that the large impacts, which occurred during the latest stages of heavy bombardment and excavated large basins, also significantly affected the initial thermal condition of the planet. The three largest impactors typically estimated for Mars (Hellas, Utopia, and Isidis) along with the hypothetical Tharsis impact assumed in our model are also shown in Figure 8 (see Table 3).

[20] Why should a very large impact at Tharsis result in a huge volcanic pile and not some kind of "megabasin"? In fact, the physics of very large impacts is not well understood and may be completely different than that of basin-forming impacts. For example, the huge initial crater and partially molten region formed by such an impact may not

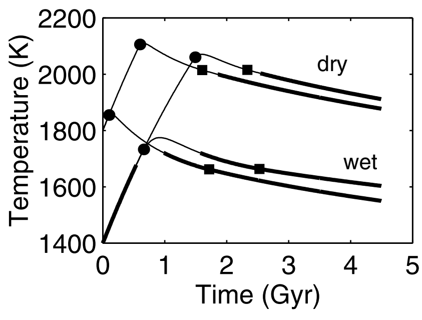

Figure 7. Stagnant lid thermal evolution as in Figure 5 including a model of differentiation (Appendix A). The circles and squares indicate the onset and cessation of convection, respectively. The evolution is characterized by a ~1–2 Gyr episode of sluggish convection, extensive melting, and nearly complete differentiation of heat-producing elements.

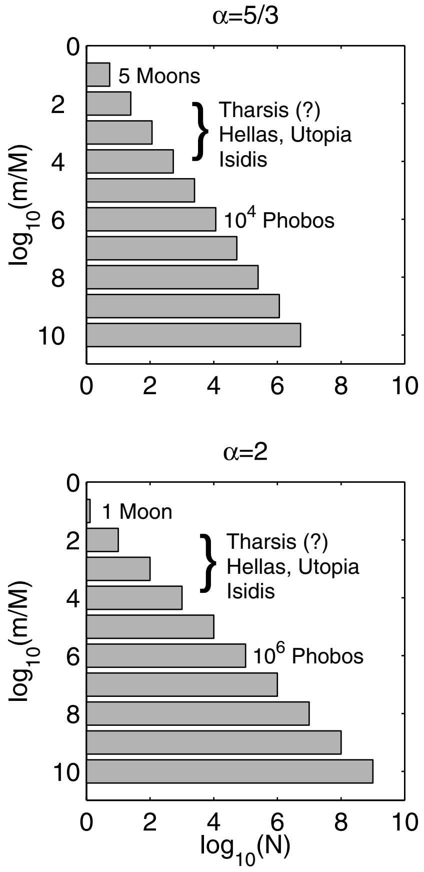

Figure 8. Illustrative inventories of planetesimals required to form Mars. For $\alpha = 2$ and 5/3, each mass decade contributes equally to the total mass and total surface area, respectively. The approximate locations of the impactors assumed in our model are also shown (see Table 3).

be preserved because of isostatic adjustment. Perhaps, there is an upper limit for impactor size beyond which a typical basin does not form. Could Tharsis represent an intermediate case between an impact basin and formation of a global magma ocean? Future studies of very large impacts might help to evaluate the soundness of this hypothesis.

5. Evolution of Impact-Induced Thermal Anomalies

[21] Fully three-dimensional spherical shell simulations of mantle convection [*Reese et al.*, 1999a] were utilized to study the thermal evolution of Mars with initial, impact-induced thermal heterogeneity.

5.1. Mantle Viscosity

[22] We assume a Newtonian viscosity ($n = 1$) and make the Frank–Kamenetskii approximation,

$$\eta = b \exp(-\gamma T), \tag{9}$$

where b and γ are constant. The nature of this approximation is that at large viscosity contrasts, the differences between the Arrhenius and exponential laws are unimportant for determining the interior temperature [*Reese et al.*, 1999b]. A rigid upper surface and $\gamma = 4 \times 10^{-3}$ ensures stagnant lid convection [*Solomatov and Moresi*, 2000].

5.2. Initial Conditions

[23] Prior to impact heating (Table 3), the nominal initial mantle temperature is assumed to be 1500 K with a fixed surface temperature of 220 K. Clearly this spherical symmetry is a first order approximation as the mantle temperature might be affected by earlier impacts, core formation, and previous mantle dynamics (see sections 1 and 2.1). The maximum initial boundary layer thickness is controlled by the accretion timescale (~30 Myr), $\delta_0 \sim 2\,(\kappa t)^{1/2}$. Due to numerical resolution restrictions we must consider a thicker boundary layer of ~500 km. Convective boundary layer instabilities develop at the critical Rayleigh number $\mathrm{Ra_{cr}} = (\rho\alpha g \Delta T \delta_0^3/\kappa\eta_i) \approx 21\,(\gamma(T_i - T_s))^4$.

5.3. Internal Heating

[24] The mantle is internally heated at an exponentially decreasing rate and the heat flux through the core–mantle boundary is assumed to be negligible. The heat production is

$$H(t) = C_d \sum_{i=1}^{4} H_{i,0} \exp[-\lambda_i (t - t_0)], \tag{10}$$

where $H_{i,0}$ are the present-day heat production values for the four major isotopes ^{235}U, ^{238}U, ^{232}Th, ^{40}K, and C_d is the depletion factor relative to the chondritic value. We assume $C_d = 0.5$ implying a strong initial fractionation of heat-producing elements in the crust and isotopic ratios of K/U = 10^4 and Th/U = 3.8. The abundance of U is chondritic, 20 ppb.

5.4. Impact Heating

[25] High speed impacts generate a compressional shock wave that propagates into the planet heating the interior while dropping off rapidly in amplitude away from the impact site [*Melosh*, 1990; *Tonks and Melosh*, 1992, 1993]. For a vertically incident impactor of radius a, the radial distance, R, corresponding to a temperature increase of ~300 K can be calculated (Appendix B, Table 3, and Figure 9). Temperatures near the impact site are much higher and limited by melting and vaporization. Since we cannot model energy dissipation via these mechanisms and are interested in long-term effects of impact heating, we assume a constant temperature increase of 300 K. Impacts also reduce the lithospheric thickness by a factor of two. Highly oblique impacts complicate this geometry, concentrating energy downrange at shallower depths [*Pierazzo and Melosh*, 2000].

5.5. Results

[26] Three models are considered. Model A is a low interior viscosity ($\eta_i \sim 3 \times 10^{22}$ Pa s) end-member with a

Table 3. Impact Heating

Impact	a (km)	R (km)
Tharsis (?)	600	1600
Utopia	250	700
Hellas	250	700
Isidis	150	400

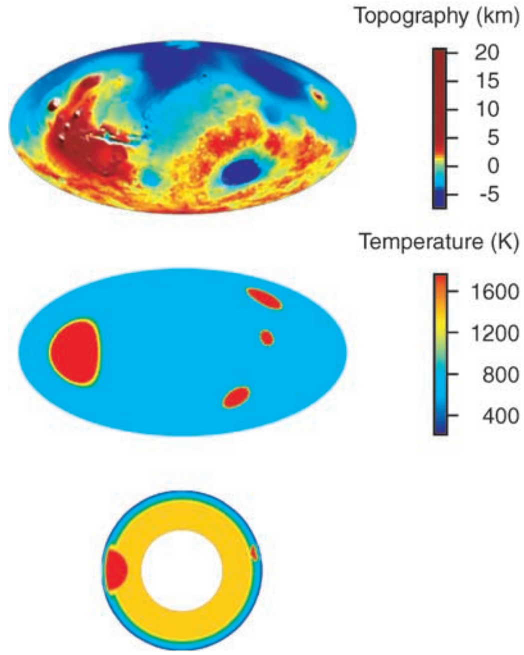

Figure 9. Martian topography (top) and initial model thermal conditions at midlithosphere depth (middle) and along a cross section (bottom) through 90°W–270°W.

convectively unstable mantle, Model B has an intermediate interior viscosity ($\eta_i \sim 10^{23}$ Pa s), and Model C is a high interior viscosity ($\eta_i > 10^{24}$ Pa s) end-member for which the evolution is purely conductive. Initially, geoid highs are strongly correlated with individual impacts. For model A, vigorous, small-scale convection quickly removes initial thermal heterogeneity due to impacts and the geoid maximum decays from ~3 km to ~300 m in 1.5 Gyr and fluctuates about this value for the remainder of evolution. The present-day, model geoid bears no resemblance to observation. Initially, convection in model B is extremely sluggish. Near the end of evolution, lithospheric instabilities begin to develop near the lowest viscosity regions. Present-day geoid highs of ~1.5 km are correlated with individual impacts. Heat transfer in model C is by conduction. Density anomalies associated with hot regions dissipate via diffusion. After 4.5 Gyr, there is a geoid high of ~1 km associated with Tharsis and a broad secondary high of ~300 m in the eastern hemisphere. Long-wavelength (hemispheric scale) features of the Model C geoid are in reasonable agreement with observational data (Figure 10).

5.6. Discussion

[27] The seemingly impressive fit of Model C to observation is, in fact, quite fortuitous. The result should not be interpreted as implying that the simple mechanism investigated here is the only contributor to Mars topography and gravity. The amplitude of geoid anomalies, but not the pattern, depends on the degree of heating and lithospheric thinning due to impacts (section 5.4). Much as in the plume hypothesis, positive geoid anomalies in the model are due solely to an upward surface deformation which, in Model C, accounts for only ~3 km of topography at Tharsis. Clearly, the remaining topography must be associated with other processes. Volcanic construction, crustal thickening, a chemically buoyant residuum in the underlying mantle, and flexural support of part of the load all have important implications for Tharsis topography and gravity. Smaller-scale features including the massive Hellas basin, material excavated from Hellas, the Isidis mascon, Valles Marineris, and volcanic shields at Tharsis and Elysium also contribute to the geoid [*Smith et al.*, 1999b; *Zuber et al.*, 2000].

[28] However, the results presented here do suggest that long-lived deep thermal heterogeneities in the mantle can play an important role. At interior viscosities higher than about 10^{23} Pa s, planetary evolution is dominated by thermal diffusion. In this limit, the results do not depend on the rheological law, which has always been an unknown in convective models of the Martian interior. Yet, convection can still play some secondary role in planetary evolution. For example, volcanic and tectonic events at Tharsis [e.g., *Anderson et al.*, 1998; *Dohm et al.*, 2000] might be related to episodic, localized convection in a partially molten mantle.

[29] Finally, the results reveal the possibility of a scenario (that can be explored in future studies) in which initial impact-induced heating, melting and differentiation are so substantial that large density variations are created not only due to temperature but also due to composition. This, and a high mantle viscosity, would ensure a purely conductive evolution. Density anomalies in the mantle would be located in exactly the same places as in the models presented here and would produce a very similar geoid pattern. An important difference from purely thermal models is that the geoid would change much less with time since there would be little "density diffusion." Independent constraints on the evolution of the geoid with time would help to constrain the relative thermal and compositional contributions to density heterogeneities in the Martian mantle.

6. Conclusions

[30] 1. Rheological constraints suggest that the Martian mantle probably evolved in the stagnant lid regime. In this case, initiation of convection can be delayed, convection is sluggish and inefficient, and extensive melting and differentiation are unavoidable. Convection might be restricted to a 1–2 Gyr episode during planetary evolution.

[31] 2. In the absence of vigorous convection, the early heterogeneous thermal state of the mantle could be preserved. One mechanism capable of locally heating the deep mantle is large impacts at the end of heavy bombardment. If such thermal anomalies are long-lived, they could affect the magmatic and tectonic evolution and even contribute to the present-day topography and gravity.

[32] 3. Plume development on Mars might be difficult due to mantle heating in the stagnant lid regime. We suggest that Tharsis may be related to a large, impact-induced, thermal anomaly rather than a convective plume. While the global thermal evolution could be dominated by conduction, episodes of Tharsis tectonism and magmatism might be associated with localized convection in a partially molten mantle.

[33] 4. There are several outstanding problems whose solutions may help further our understanding of Martian

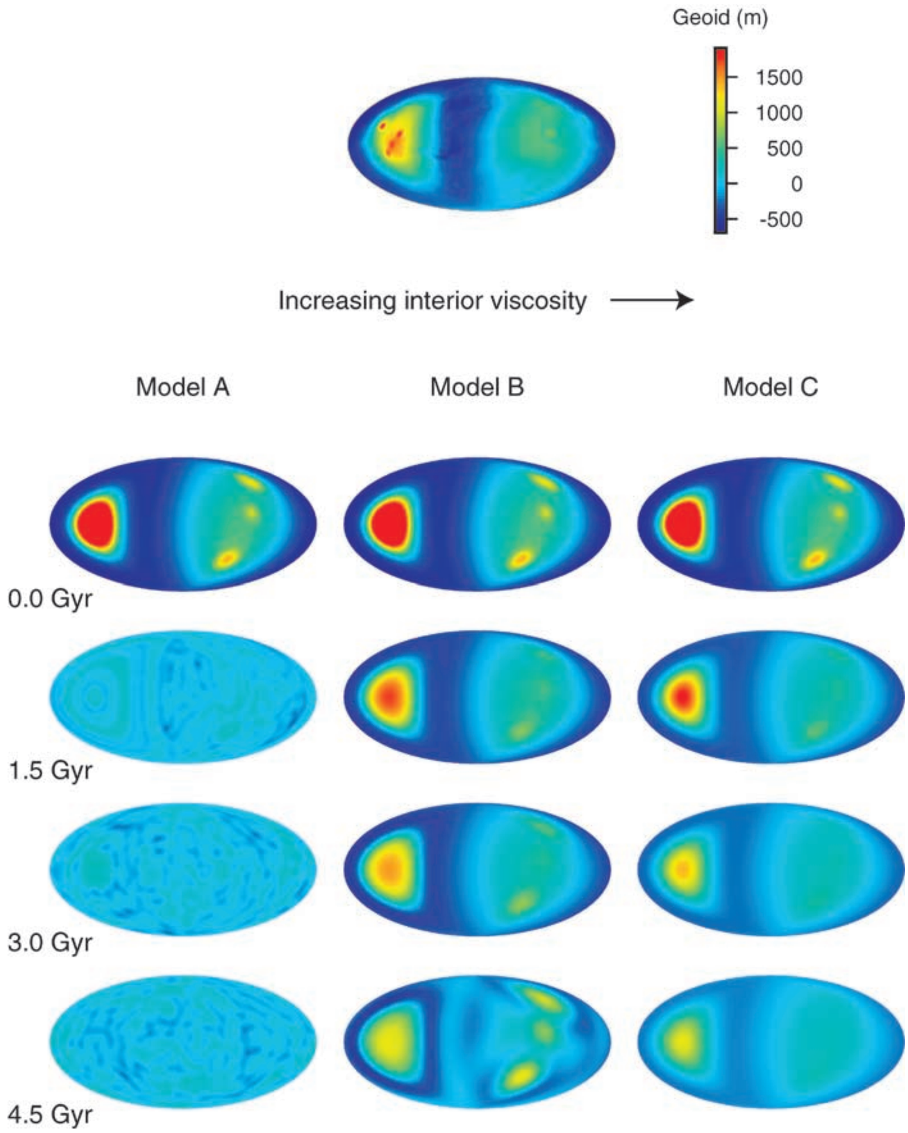

Figure 10. The present-day geoid (top) as measured by MGS and the geoid evolution for the three models at 0.0, 1.5, 3.0, and 4.5 Gyr. In the low interior viscosity model (A), initial thermal heterogeneity is quickly eliminated by vigorous convection. For the intermediate viscosity model (B), convection is confined to impact-heated regions. Sufficiently high interior viscosity (C) ensures a purely conductive thermal evolution and gives the best agreement with observation.

thermal evolution. The initial condition is an unresolved issue. Better constraints on Martian core formation and early temperature profile would help constrain the initial convective state of the mantle. Large impact physics is not well understood. It seems the parameter space of interest is that between basin-forming impacts and giant impacts that melt the entire planet. If Tharsis is the surface manifestation of such an impact, data returned by MGS might reveal characteristic geological and geophysical signatures in and around the plateau. If the mantle is indeed pyroxene rich, a more complete description of pyroxene rheology is necessary. The activation volume is not known and yet plays an important role in determining stagnant lid heat transfer efficiency. Further constraints could be placed on the model by extending it to track the distribution of magmatism with time. Results could then be directly compared to the volcanic history which, in general, has evolved from widespread activity, including episodes of plains volcanism, to more localized activity at centers of volcanic construction, including Tharsis and Elysium [*Tanaka et al.*, 1992]. The model results could also be compared to estimates of crustal thickness [*Zuber et al.*, 2000]. Finally, models, which address compositional density anomalies due to melting and differentiation associated with large impacts, should also be considered. In this case, relative contributions from thermal and compositional anomalies could be constrained with observational data on geoid evolution.

Appendix A: Melting and Differentiation

[34] The solidus is constrained by experimental data for peridotite [*McKenzie and Bickle*, 1988; *Scarfe and Takaha-*

shi, 1986; *Ito and Takahashi*, 1987]. The solidus is parameterized as

$$T_s = 1374 + 130p - 5.6p^2 \tag{A1}$$

where the temperature is in Kelvin and pressure in gigapascals. After the slope reaches dT/dp = 10 K GPa^{-1} the temperature increases linearly with pressure. The liquidus and melt fractions are given by the expressions of *McKenzie and Bickle* [1988]. Only dry melting is considered. Wet melting occurs at even lower interior temperatures.

[35] The depth range between the beginning of melting and the bottom of the stagnant lid, z_m, determines the width of the horizontal flow which underwent melting. For a cylindrical upwelling of velocity u_i in a convection cell of radius d, the rate at which material passes through this channel is simply $u_i z_m 2\pi d$ [*Reese et al.*, 1999b]. The differentiation rate is estimated as follows. If, before melting, the concentration of radioactive elements is C, the chemical flux through the partially molten region is $u_i C z_m 2\pi d$. Radioactive elements are assumed to be completely extracted, giving an estimate for the chemical loss rate from the mantle. The rate of decrease of the total amount of radioactive elements in the cylindrical convection cell is d($C\pi d^3$)/dt,

$$\frac{\mathrm{d}C}{\mathrm{d}t} \approx -2\, C \frac{z_m}{d} \frac{u}{d}, \tag{A2}$$

Appendix B: Impact Heating

[36] After the shock passes, material decompresses to ambient pressure. If the release adiabat is approximated by the Hugoniot curve, the shock heating is given by [*Melosh*, 1989]

$$\Delta T = \frac{1}{c_p} \frac{u_p^2}{2} \left[1 - 2\left(\xi - \xi^2 \ln(1 + 1/\xi)\right)\right], \tag{B1}$$

where $\xi = C/(Su_p)$, C and S are material parameters, and the particle velocity (material velocity behind the shock front)

$$u_p(r) = \begin{cases} u_{p0} & r < r_0 \\ u_{p0}(r_0/r)^2 & r > r_0 \end{cases}. \tag{B2}$$

The particle velocity in the core

$$u_{p0} = \chi v \cos\theta \tag{B3}$$

where v and θ are the impact velocity and angle, respectively and the parameter χ is found from impedance matching [*Melosh*, 1989]. Near the impact site there is a region that is shocked to approximately uniform pressure. The radius of this isobaric core

$$r_0 = \left(\frac{\rho_p v^2}{2\rho_t u_{p0}^2}\right) a, \tag{B4}$$

where a is the impactor radius and ρ_p and ρ_t are the projectile and target densities, respectively. We assume vertical incidence $\theta = 0$ and $\rho_p = \rho_t$ implying $\chi = 1/2$. In this case, to first nonvanishing order in ξ, (B1) gives the radius R corresponding to temperature increase ΔT,

$$R = \left(\frac{8Sv^3}{3Cc_p\Delta T}\right)^{1/6} a \tag{B5}$$

For C = 6.6 km/s and S = 0.9 [*Melosh*, 1989], v = 10 km/s and ΔT = 300 K, the coefficient is ~3 (see Table 3).

[37] **Acknowledgment.** This work was supported by NASA grants NAG5-8803 and NAG5-10578 and NUCOR program at Los Alamos National laboratory.

References

Abe, Y., and T. Matsui, The formation of an impact-generated H_2O atmosphere and its implication for the early thermal history of the Earth, *Proc. Lunar Planet. Sci. Conf. 15th*, Part 2, *J. Geophys. Res.*, *90*, suppl., C545–C559, 1985.

Acuña, M. H., J. E. P. Connerney, N. F. Ness, R. P. Lin, D. Mitchell, C. W. Carlson, J. McFadden, K. A. Anderson, H. Rème, and C. Mazelle, Global distribution of crustal magnetization discovered by the Mars Global Surveyor MAG/ER experiment, *Science*, *284*, 790–793, 1999.

Agnor, C. B., R. M. Canup, and H. F. Levison, On the character and consequences of large impacts in the late stage of terrestrial planet formation, *Icarus*, *142*, 219–237, 1999.

Albarède, F., J. Blichert-Toft, J. D. Vervoort, J. D. Gleason, and M. Rosing, Hf-Nd isotope evidence for a transient dynamic regime in the early terrestrial mantle, *Nature*, *404*, 488–490, 2000.

Anderson, R. C., M. P. Golombek, B. J. Franklin, K. L. Tanaka, J. M. Dohm, J. H. Lias, and B. Peer, Centers of tectonic activity through time for the Western Hemisphere of Mars, *Lunar Planet. Sci. Conf.*, *29*, 1881, 1998.

Avé Lallemant, H. G., Experimental deformation of diopside and websterite, *Tectonophysics*, *48*, 1–27, 1978.

Baker, V. R., M. H. Carr, V. C. Gulick, C. R. Williams, and M. S. Marley, Channels and valley networks, in *Mars*, edited by H. H. Kieffer et al., pp. 493–522, Univ. of Ariz. Press, Tucson, 1992.

Banerdt, W. B., and M. P. Golombek, Tectonics of the Tharsis region of Mars: Insights from MGS topography and gravity, *Lunar Planet. Sci. Conf.*, *31*, 2038, 2000.

Bertka, C. M., and Y. W. Fei, Density profile of an SNC model Martian interior and the moment of inertia factor of Mars, *Earth Planet. Sci. Lett.*, *157*, 79–88, 1998a.

Bertka, C. M., and Y. W. Fei, Implication of Mars Pathfinder data for the accretion history of the terrestrial planets, *Science*, *281*, 1838–1840, 1998b.

Bertka, C. M., and Y. W. Fei, Geophysical and geochemical constraints on the composition and structure of the Martian interior, *5th Int. Mars Conf.*, 6225, 1999.

Breuer, D., D. A. Yuen, T. Spohn, and S. Zhang, Three dimensional models of Martian mantle convection with phase transitions, *Geophys. Res. Lett.*, *25*, 229–232, 1998.

Bruhn, D., N. Groebner, and D. L. Kohlstedt, An interconnected network of core-forming melts produced by shear deformation, *Nature*, *403*, 883–886, 2000.

Carr, M. H., Tectonism and volcanism of the Tharsis region of Mars, *J. Geophys. Res.*, *79*, 3943–3949, 1974.

Carr, M. H., *Water on Mars*, Oxford Univ. Press, New York, 1996.

Carr, M. H., and H. Wänke, Earth and Mars: Water inventories as clues to accretional histories, *Icarus*, *98*, 61–71, 1992.

Connerney, J. E. P., M. H. Acuña, J. Wasilewski, N. F. Ness, H. Rème, C. Mazelle, D. Vignes, R. P. Lin, D. L. Mitchell, and P. A. Cloutier, Magnetic lineations in the ancient crust of Mars, *Science*, *284*, 794–798, 1999.

Coradini, A., C. Federico, and P. Lanciano, Earth and Mars: Early thermal profiles, *Phys. Earth. Planet. Inter.*, *31*, 145–160, 1983.

Davaille, A., and C. Jaupart, Transient high Rayleigh number thermal convection with large viscosity variations, *J. Fluid Mech.*, *253*, 141–166, 1993.

Dohm, J. M., R. C. Anderson, V. R. Baker, R. G. Strom, G. Komatsu, and T. M. Hare, Pulses of magmatic activity through time: Potential triggers for climatic variations on Mars, *Lunar Planet. Sci. Conf.*, *31*, 1632, 2000.

Doin, M.-P., L. Fleitout, and U. Christensen, Mantle convection and stability of depleted and undepleted continental lithosphere, *J. Geophys. Res.*, *102*, 2771–2787, 1997.

Dreibus, G., and H. Wänke, Volatiles on Earth and Mars: A comparison, *Icarus*, *71*, 225–240, 1987.

Fallick, A. E., R. W. Hinton, D. P. Mattey, S. J. Norris, C. T. Pillinger, P. K. Swart, and I. P. Wright, No unusual compositions of the stable isotopes of nitrogen, carbon, and hydrogen in SNC meteorites, *Lunar Planet. Sci. Conf.*, *14*, 183–184, 1983.

Folkner, W. M., C. F. Yoder, D. N. Yuan, E. M. Standish, and R. A. Preston, Interior structure and seasonal mass redistribution of Mars from radio tracking of Mars Pathfinder, *Science*, *278*, 1749–1752, 1997.

Fowler, A. C., Fast thermoviscous convection, *Stud. Appl. Math.*, *72*, 1–34, 1985.

Gaetani, G. A., and T. L. Grove, Partitioning of moderately siderophile elements among olivine, silicate melt, and sulfide melt: Constraints on core formation in the Earth and Mars, *Geochim. Cosmochim. Acta*, *61*, 1829–1846, 1997.

Grasset, O., and E. M. Parmentier, Thermal convection in a volumetrically heated, infinite Prandtl number fluid with strongly temperature-dependent viscosity: Implications for planetary evolution, *J. Geophys. Res.*, *103*, 18,171–18,181, 1998.

Greeley, R., Release of juvenile water on Mars: Estimated amounts and timing associated with volcanism, *Science*, *236*, 1653–1654, 1987.

Grimm, R. E., and H. Y. McSween, Heliocentric zoning of the asteroid belt by Al-26 heating, *Science*, *259*, 653–655, 1993.

Harder, H., Mantle convection and the dynamic geoid of Mars, *Geophys. Res. Lett.*, *27*, 301–304, 2000.

Harder, H., and U. R. Christensen, A one-plume model of Martian mantle convection, *Nature*, *380*, 507–509, 1996.

Hartmann, W. K., Martian surface and crust: Review and synthesis, *Icarus*, *19*, 550–575, 1973.

Hartmann, W. K., M. Malin, A. MvEwen, M. Carr, L. Soderblom, P. Thomas, E. Danielson, P. James, and J. Veverka, Evidence for recent volcanism on Mars from crater counts, *Nature*, *397*, 586–589, 1999a.

Hartmann, W. K., D. C. Berman, G. A. Esquerdo, and A. MvEwen, Recent Martian volcanism: New evidence from Mars Global Surveyor, *Lunar Planet. Sci. Conf.*, *30*, 1270, 1999b.

Hauck, S. A., and R. J. Phillips, Mars dirty little secret, *Lunar Planet. Sci. Conf.*, *31*, 1303, 2000.

Head, J. W., H. Hiesenger, M. A. Ivanov, M. A. Kreslavsky, S. Pratt, and B. J. Thompson, Possible ancient oceans on Mars: Evidence from Mars Orbiter Laser Altimeter data, *Science*, *286*, 2134–2137, 1999.

Ito, E., and E. Takahashi, Melting of peridotite at uppermost lower-mantle conditions, *Nature*, *328*, 514–517, 1987.

Johnson, M. C., M. J. Rutherford, and P. C. Hess, Chassigny petrogenesis: Melt compositions, intensive parameters, and water contents of Martian magmas, *Geochim. Cosmochim. Acta*, *55*, 349–366, 1991.

Karato, S.-I., Does partial melting reduce the creep strength of the upper mantle?, *Nature*, *319*, 8151–8176, 1986.

Karato, S.-I., and P. Wu, Rheology of the upper mantle: A synthesis, *Science*, *260*, 771–778, 1993.

Karato, S.-I., and V. R. Murthy, Core formation and chemical equilibrium in the Earth, I, Physical considerations, *Phys. Earth Planet. Inter.*, *100*, 61–79, 1997.

Karlsson, H. R., R. N. Clayton, E. K. Gibson, T. K. Mayeda, and R. A. Socki, Water in SNC meteorites: Evidence for a Martian hydrosphere, *Science*, *255*, 1409–1411, 1992.

Kaula, W. M., Thermal evolution of Earth and moon growing by planetesimal impacts, *J. Geophys. Res.*, *84*, 999–1008, 1979.

Keil, K., Thermal alteration of asteroids: Evidence from meteorites, *Planet. Space Sci.*, *48*, 887–903, 2000.

Kerridge, J. F., Deuterium in Shergotty and Lafayette (and on Mars?), *Lunar Planet. Sci. Conf.*, *19*, 599–600, 1988.

Lee, D. C., and A. N. Halliday, Core formation on Mars and differentiated asteroids, *Nature*, *388*, 854–857, 1997.

Malin, M. C., and K. S. Edgett, Evidence for recent groundwater seepage and surface runoff on Mars, *Science*, *288*, 2330–2335, 2000.

Mackwell, S. J., High temperature rheology of enstatite: Implications for creep in the mantle, *Geophys. Res. Lett.*, *18*, 2027–2030, 1991.

McEwen, A. S., M. C. Malin, M. H. Carr, and W. K. Hartmann, Voluminous volcanism on early Mars revealed in Valles Marineris, *Nature*, *397*, 584–586, 1999.

McKenzie, D., and M. J. Bickle, The volume and composition of melt generated by extension of the lithosphere, *J. Petrol.*, *29*, 625–679, 1988.

McSween, H. Y., and R. P. Harvey, Outgassed water on Mars: Constraints from melt inclusions in SNC meteorites, *Science*, *259*, 1890–1892, 1993.

Melosh, H. J., *Impact Cratering: A Geological Process*, Oxford Univ. Press, New York, 1989.

Melosh, H. J., Giant impacts and thermal state of the early Earth, in *Origin of the Earth*, edited by H. E. Newsom and J. H. Jones, pp. 69–84, Oxford Univ. Press, New York, 1990.

Moresi, L.-N., and V. S. Solomatov, Numerical investigation of 2D convection with extremely large viscosity variations, *Phys. Fluids*, *7*, 2154–2162, 1995.

Morris, S., and D. Canright, A boundary-layer analysis of Benard convection in a fluid of strongly temperature-dependent viscosity, *Phys. Earth Planet. Inter.*, *36*, 355–373, 1984.

Nimmo, F., Dike intrusion as a possible cause of linear Martian magnetic anomalies, *Geology*, *28*, 391–394, 2000.

Nimmo, F., and D. Stevenson, The influence of early plate tectonics on the thermal evolution and magnetic field of Mars, *J. Geophys. Res.*, *105*, 11,969–11,979, 2000.

Ogawa, M., G. Schubert, and A. Zebib, Numerical simulations of three-dimensional thermal convection in a fluid with strongly temperature-dependent viscosity, *J. Fluid Mech.*, *233*, 299–328, 1991.

Pierazzo, E., and H. J. Melosh, Melt production in oblique impacts, *Icarus*, *145*, 252–261, 2000.

Pierazzo, E., A. M. Vickery, and H. J. Melosh, A reevaluation of impact melt production, *Icarus*, *127*, 408–423, 1997.

Pruis, M. J., and K. L. Tanaka, The Martian northern plains did not result from plate tectonics, *Lunar Planet. Sci. Conf.*, *26*, 1147–1148, 1995.

Phillips, R. J., and E. R. Ivins, Geophysical observations pertaining to solid-state convection in the terrestrial planets, *Phys. Earth Planet. Inter.*, *19*, 107–148, 1979.

Phillips, R. J., M. T. Zuber, S. A. Hauck, R. M. Williams, and K. B. Portle, Why is there a negative gravity ring around Tharsis on Mars?, *Lunar Planet. Sci. Conf.*, *31*, 1303, 2000.

Purucker, M., D. Ravat, H. Frey, C. Voorhies, T. Sabaka, and M. Acuña, An altitude-normalized magnetic map of Mars and its interpretation, *Geophys. Res. Lett.*, *27*, 2452–2499, 2000.

Raymond, C. A., E. Smrekar, and E. R. Stofan, Sources of magnetic anomalies and their implications, *Lunar Planet. Sci. Conf.*, *31*, 2062, 2000.

Reese, C. C., V. S. Solomatov, and L.-N. Moresi, Heat transport efficiency for stagnant lid convection with dislocation viscosity: Application to Mars and Venus, *J. Geophys. Res.*, *103*, 13,643–13,657, 1998.

Reese, C. C., V. S. Solomatov, J. R. Baumgardner, and W.-S. Yang, Stagnant lid convection in a spherical shell, *Phys. Earth Planet. Inter.*, *116*, 1–7, 1999a.

Reese, C. C., V. S. Solomatov, and L.-N. Moresi, Non-Newtonian stagnant lid convection and magmatic resurfacing on Venus, *Icarus*, *139*, 67–80, 1999b.

Ross, J. V., and K. C. Nielsen, High temperature flow of wet polycrystalline enstatite, *Tectonophysics*, *44*, 233–261, 1978.

Rushmer, T., W. G. Minarik, and G. J. Taylor, Physical processes of core formation, in *Origin of the Earth and Moon*, edited by R. Canup and K. Righter, pp. 227–244, Univ. of Ariz. Press, Tucson, 2000.

Safronov, V. S., The heating of the earth during its formation, *Icarus*, *33*, 1–12, 1978.

Sanloup, C., A. Jambon, and P. Gillet, A simple chondritic model of Mars, *Phys. Earth Planet. Inter.*, *112*, 43–54, 1999.

Sasaki, S., and K. Nakazawa, Metal-silicate fractionation in the growing Earth: Energy source for the terrestrial magma ocean, *J. Geophys. Res.*, *91*, 9231–9238, 1986.

Scarfe, C. M., and E. Takahashi, Melting of garnet peridotite to 13 GPa and the early history of the upper mantle, *Nature*, *322*, 354–356, 1986.

Schubert, G., and T. Spohn, Thermal evolution of Mars and the sulfur content of its core, *J. Geophys. Res.*, *95*, 14,095–14,104, 1990.

Schubert, G., D. L. Turcotte, and E. R. Oxburgh, Stability of planetary interiors, *Geophys. J. R. Astron. Soc.*, *18*, 441–460, 1969.

Schubert, G., P. Cassen, and R. E. Young, Subsolidus convective cooling histories of terrestrial planets, *Icarus*, *38*, 192–211, 1979.

Schubert, G., S. C. Solomon, D. L. Turcotte, M. J. Drake, and N. H. Sleep, Origin and thermal evolution of Mars, in *Mars*, edited by H. H. Kieffer et al., pp. 147–183, Univ. of Ariz. Press, Tucson, 1992.

Schultz, P. H., Impact basin control of volcanic and tectonic provinces on Mars, *Lunar Planet. Sci. Conf.*, *14*, 728–729, 1984.

Schultz, P. H., and H. Glicken, Impact crater and basin control of igneous processes on Mars, *J. Geophys. Res.*, *84*, 8033–8047, 1979.

Schultz, R. A., and H. V. Frey, A new survey of large multiring impact basins on Mars, *J. Geophys. Res.*, *95*, 14,175–14,189, 1990.

Sleep, N. H., Martian plate tectonics, *J. Geophys. Res.*, *99*, 5639–5655, 1994.

Smith, D., et al., The global topography of Mars and implications for surface evolution, *Science*, *284*, 1495–1503, 1999a.

Smith, D. E., W. L. Sjogren, G. L. Tyler, G. Balmino, F. G. Lemoine, and A. S. Konopliv, The gravity field of Mars: Results from Mars Global Surveyor, *Science*, *286*, 94–97, 1999b.

Solomatov, V. S., Scaling of temperature and stress dependent viscosity convection, *Phys. Fluids*, *7*, 266–274, 1995.

Solomatov, V. S., and L.-N. Moresi, Time dependent stagnant lid convection on the Earth and other terrestrial planets, *J. Geophys. Res.*, *105*, 21,795–21,817, 2000.

Solomon, S. C., Formation, history and energetics of cores in the terrestrial planets, *Phys. Earth Planet. Inter.*, *19*, 168–182, 1979.
Solomon, S. C., and J. Chaiken, Thermal expansion and thermal stress in the Moon and terrestrial planets: Clues to early thermal history, *Proc. Lunar Sci. Conf.*, *7*, 3229–3243, 1976.
Solomon, S. C., and J. W. Head, Evolution of the Tharsis province of Mars: The importance of heterogeneous lithospheric thickness and volcanic construction, *J. Geophys. Res.*, *82*, 9755–9774, 1982.
Solomon, S. C., et al., Lithospheric structure from Mars Global Surveyor topography and gravity and implications for the early thermal evolution of Mars, *Lunar Planet. Sci. Conf.*, *31*, 1808, 2000.
Spohn, T., Mantle differentiation and thermal evolution of Mars, Mercury, and Venus, *Icarus*, *90*, 222–236, 1991.
Spohn, T., F. Sohl, and D. Breuer, Mars, *Astron. Astrophys. Rev.*, *8*, 181–235, 1998.
Stevenson, D. J., Models of the Earth's core, *Science*, *214*, 611–619, 1981.
Stevenson, D. J., Fluid dynamics of core formation, in *Origin of the Earth*, edited by H. E. Newsom and J. H. Jones, Oxford Univ. Press, New York, 1990.
Stevenson, D. J., T. Spohn, and G. Schubert, Magnetism and thermal evolution of the terrestrial planets, *Icarus*, *54*, 466–489, 1983.
Tajika, E., and S. Sasaki, Magma generation on Mars constrained from ^{40}Ar degassing model, *J. Geophys. Res.*, *101*, 7543–7554, 1996.
Tanaka, K. L., D. H. Scott, and R. Greeley, Global stratigraphy, in *Mars*, edited by H. H. Kieffer et al., pp. 345–382, Univ. of Ariz. Press, Tucson, 1992.
Thompson, A. B., Water in the Earth's upper mantle, *Nature*, *358*, 295–302, 1992.
Toksöz, M. N., A. T. Hsui, and D. H. Johnston, Thermal evolutions of the terrestrial planets, *Moon Planets*, *18*, 265–276, 1978.
Tonks, W. B., and H. J. Melosh, Core formation by giant impacts, *Icarus*, *100*, 326–346, 1992.
Tonks, W. B., and H. J. Melosh, Magma ocean formation due to giant impacts, *J. Geophys. Res.*, *98*, 5319–5333, 1993.
Tozer, D. C., Heat Transfer and convection currents, *Philos. Trans. R. Soc. London, Ser. A*, *258*, 252–271, 1965.
Tozer, D. C., The present thermal state of the terrestrial planets, *Phys. Earth Planet. Inter.*, *6*, 182–187, 1972.
Trompert, R. A., and U. Hansen, On the Rayleigh number dependence of convection with a strongly temperature-dependent viscosity, *Phys. Fluids*, *10*, 351–360, 1998.
Turcotte, D. L., Thermal evolution of Mars and Venus including irreversible fractionation, *Lunar Planet. Sci. Conf.*, *20*, 1138–1139, 1989.
Turcotte, D. L., and E. R. Oxburgh, Finite amplitude convection cells and continental drift, *J. Fluid Mech.*, *28*, 29–42, 1967.
Turcotte, D. L., F. A. Cooke, and R. J. Willeman, Parameterized convection within the Moon and terrestrial planets, *Lunar Planet. Sci. Conf.*, *10*, 2375–2392, 1979.
Weidenschilling, S. J., D. Spaute, D. R. Davis, F. Marzari, and K. Ohtsuki, Accretional evolution of a planetesimal swarm, 2, The terrestrial zone, *Icarus*, *126*, 429–455, 1997.
Weinstein, S. A., The effects of a deep mantle endothermic phase change on the structure of thermal convection in silicate planets, *J. Geophys. Res.*, *100*, 11,719–11,728, 1995.
Wetherill, G. W., Formation of the terrestrial planets, *Annu. Rev. Astron. Astrophys.*, *18*, 77–113, 1980.
Wetherill, G. W., Formation of the Earth, *Annu. Rev. Earth Planet. Sci.*, *18*, 205–256, 1990.
Yang, J., and S. Epstein, A study of stable isotopes in Shergotty meteorite, *Lunar Planet. Sci. Conf.*, *26*, 25–26, 1985.
Zahnle, K. J., J. G. Kasting, and J. B. Pollack, Evolution of a steam atmosphere during Earth's accretion, *Icarus*, *74*, 62–97, 1988.
Zuber, M. T., et al., Internal structure and early thermal evolution of Mars from Mars Global Surveyor topography and gravity, *Science*, *287*, 1788–1793, 2000.

J. R. Baumgardner, Theoretical Division, MS B216, Los Alamos National Laboratory, Los Alamos, NM 87545, USA. (johnrb@lanl.gov)
C. C. Reese and V. S. Solomatov, Department of Physics, New Mexico State University, Las Cruces, NM 88003, USA. (creese@nmsu.edu; slava@nmsu.edu)